

Production of Regional 1 km × 1 km Water Vapor Fields through the Integration of GPS and MODIS Data

Zhenhong Li
Department of Geomatic Engineering
University College London, UK

BIOGRAPHY

Zhenhong Li is a PhD student at the Department of Geomatic Engineering at University College London, UK. His main research interests are correction of atmospheric water vapor effects on repeat-pass SAR interferometry using GPS, MODIS and MERIS data, and he specializes in atmospheric water vapor. Zhenhong received a B.Sc. in Geodesy from Wuhan Technical University of Surveying and Mapping (WTUSM) in 1997. He holds an Overseas Research Students Award (ORS) and a UCL Graduate School Research Scholarship from 2001 to 2004.

ABSTRACT

Atmospheric water vapor is a crucial element in weather, climate and hydrology. With the recent advance in Global Positioning System (GPS) Meteorology, ground-based GPS has become an operational tool that can measure precipitable water vapor (PWV) with high accuracy (1~1.5mm) during all-weather, and with high temporal resolution (e.g. 5 minutes) at low cost. But the spatial coverage of GPS receivers is limited, and restricts its applications. At present, two NASA Moderate Resolution Imaging Spectroradiometer (MODIS) can provide global coverage 2D water vapor field with a spatial resolution of 1 km × 1 km (at nadir) every 2 days, and at many latitudes can provide water vapor fields every 90 minutes, 4 times a day. The disadvantages of MODIS water vapor products are: 1). A systematic uncertainty of 5-10% is expected [Gao *et al.*, 2003; Li *et al.*, 2003]; 2). Since the MODIS water vapor retrieval relies on observations of water vapor attenuation of near Infrared (IR) solar radiation reflected by surfaces and clouds, it is sensitive to the presence of clouds. The frequency and the percentage of cloud free conditions at mid-latitudes is only 15-30% on average [Li *et al.*, 2004]. Therefore, in order to extract a water vapor field above the Earth's surface, an attempt needs to be made to fill in the cloudy pixels.

In this paper, an inter-comparison between MODIS (collection 4) and GPS PWV products was performed in the region of the Southern California Integrated GPS

Network (SCIGN). It is shown that MODIS appeared to overestimate PWV against GPS with a scale factor of 1.05 and a zero-offset of -0.7 mm. Taking into account the small standard deviation of the linear fit model, a GPS-derived correction linear fit model was proposed to calibrate MODIS PWV products, and a better agreement was achieved. In order to produce regional 1 km × 1 km water vapor fields, an integration approach was proposed: Firstly, MODIS near IR water vapor was calibrated using GPS data; secondly, an improved inverse distance weighted interpolation method (IIDW) was applied to fill in the cloudy pixels; thirdly, the densified water vapor field was validated using GPS data. It is shown that the integration approach was promising. After correction, MODIS and GPS PWV agreed to within 1.6 mm in terms of standard deviations using appropriate extent and power parameters of IIDW, and the coverage of water vapor fields increased by up to 21.6%.

In addition, for the first time, spatial structure functions were derived from MODIS near IR water vapor, and large water vapor variations were observed from time to time.

1. INTRODUCTION

Water vapor is the main greenhouse gas in the atmosphere, playing a key role in the hydrological cycle, and has a fundamental impact on the Earth's climate. Therefore, knowledge of water vapor distributions is of crucial importance to the operational weather and climate forecasting.

Over the last ten years, ground-based GPS techniques have been developed as an operational tool for measuring precipitable water vapor (PWV), which has been well demonstrated and tested [Bevis *et al.*, 1992; Niell *et al.*, 2001; Li *et al.*, 2003]. Based on inter-comparisons with radiosondes and water vapor radiometers (WVRs), it has been shown that GPS PWV can be estimated with an accuracy of 1-1.5 mm. In addition to the high accuracy, the advantages of GPS lie in its high temporal resolution (e.g. 5 minutes), its all-weather capabilities, and relatively low costs. However, the spatial coverage is still the main limitation. On the one hand, only very limited GPS measurements can be collected in Polar regions or over

the oceans (if at all). On the other hand, even in the world's densest regional GPS network, the Southern California Integrated GPS Network (SCIGN), or the world's largest nationwide GPS network, Japan's GEONET, the station spacing varies from only a few kilometers to tens of kilometers, which is not sufficiently dense for many applications, particularly the one of interest here which is to correct atmospheric effects on SAR interferograms with a pixel spacing of ≤ 100 meters.

Observations from satellites offer global coverage with moderate spatial resolutions (300 m \sim 1 km) but with a lower temporal sampling. Currently, two Moderate Resolution Imaging Spectroradiometer (MODIS) instruments on board the NASA Terra and Aqua Spacecraft platforms can be used for the monitoring of water vapor using five near Infrared channels in the 0.8-1.3 μm spectral region, allowing global coverage of the Earth every 3 days. The MODIS near IR PWV is claimed to be determined with an accuracy of 5-10% with a spatial resolution of 1 km \times 1 km at nadir [Gao *et al.*, 2003]. As MODIS near IR PWV is sensitive to the presence of clouds in the field of view, only MODIS PWV values collected under cloud free conditions can be used. It should be borne in mind that both the frequency and the percentage of cloud free conditions are only 15-30% on average at mid latitudes [Li *et al.*, 2004], suggesting the applications of MODIS near IR PWV products may be limited by season and geographical location.

The purpose of this paper is to demonstrate how both the accuracy and the coverage of 2D MODIS near IR water vapor field can be improved using GPS data. Descriptions of data sources used in this paper are given in section 2. In section 3, an inter-comparison between MODIS and GPS PWV is presented along with a GPS-derived correction model to calibrate MODIS near IR water vapor products. In section 4, an improved inverse distance weighted interpolation method (IIDW) is introduced to fill in cloudy pixels, as well as validation using GPS PWV and some discussions on extent and power parameters of IIDW. A first attempt at the spatial structure function of water vapor derived from GPS-corrected MODIS near IR water vapor is presented in section 5, followed by some conclusions of this study in section 6.

2. DATA SOURCES

The area of interest is located in the region of the Southern California Integrated GPS Network (SCIGN) (33.20°-34.50°N, 117.2°-118.6°W) (Figure 1). The range of altitude is up to 3 km.

As mentioned earlier, only MODIS PWV values under cloud free conditions are applicable. Sixteen scenes of Terra MODIS near IR water vapor products with reasonable cloud free pixels ($>60\%$) were selected using the MODIS Global Land Browse image products (<http://modis-land.gsfc.nasa.gov>) to identify the presence of clouds from March 2000 to August 2003. Figure 2

shows an example of MODIS near IR water vapor field covering the test area collected at 18:50 UTC on 29 July 2000.

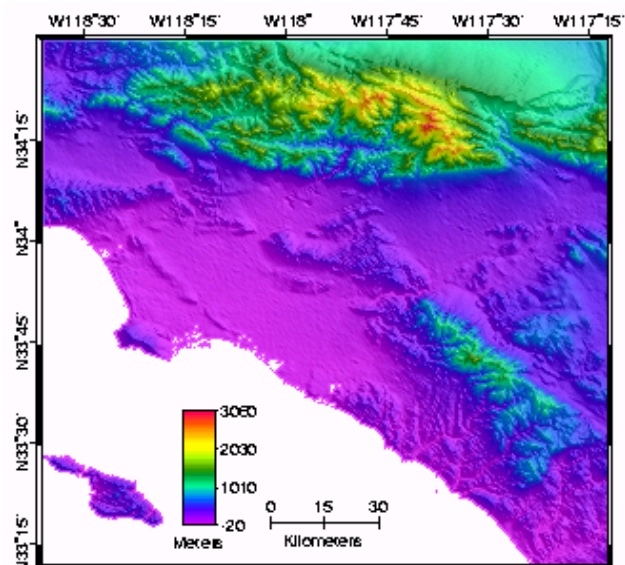


Figure 1. Hill-shaded topographic map of the area of interest produced from SRTM DEM.

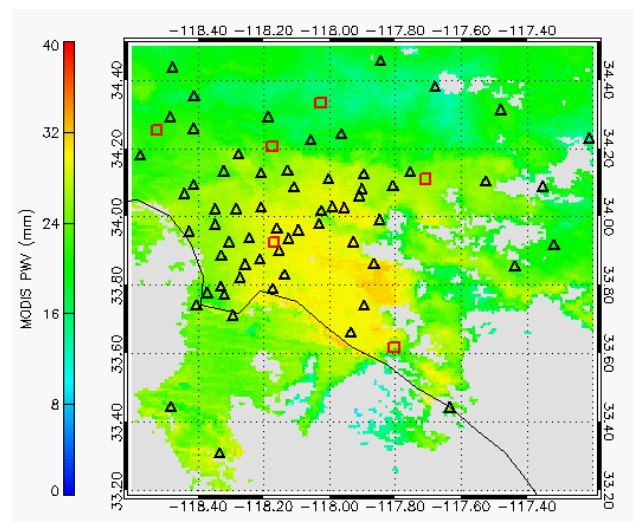


Figure 2. An example of MODIS near IR water vapor field collected at 18:50 UTC on 29 July 2000. Red squares represent GPS station with Meteorological data, and Black triangles GPS stations without Met data. The gray indicates "missing values" due to clouds.

The total number of GPS stations varied from 71 in March 2000 to 92 in August 2003 as partly shown in Figure 2. GPS data were processed in 24-hour daily solutions using the GIPSY-OASIS II software package in Precise Point Positioning mode [Zumberge *et al.*, 1997] as described in Li *et al.* [2003].

Surface pressure and temperature measurements were collected at up to 7 GPS stations. Based on the single-reference differential Berg model proposed by

Webley *et al.* [2002], an improved multi-reference differential model was proposed to derive surface pressures using all the available pressure data: Firstly, the modeled pressure was calculated using the Berg model at each station; Secondly, the difference between the observed pressures and the modeled values at each known station was calculated; Thirdly, for each unknown station, distances to all known stations were computed; Fourthly, Inverse Distance Weighted (IDW) interpolation [Shepard, 1968] was used to compute the correction value (offset) for each unknown station; Finally, the surface pressure computed at each unknown station was corrected using the offset. In order to check this multi-reference differential Berg pressure model, a time-series inter-comparison between the modeled pressures and the measured pressures was performed over the JPLM GPS station for two years. A standard deviation of 0.8 hPa was observed with a mean difference of 0.7 hPa (modeled value > measured value), suggesting that the uncertainties of modeled surface pressures might result in uncertainties of PWV of less than 0.3 mm.

A similar multi-reference differential approach was applied to fit surface temperatures except that a vertical adiabatic temperature gradient of -6.5 K/km was assumed instead of the Berg Model. The formula proposed by Bevis *et al.* [1992] was applied to convert zenith wet delay (ZWD) into PWV.

3. GPS-DERIVED CORRECTION MODEL FOR MODIS NEAR IR WATER VAPOR

A spatio-temporal inter-comparison between MODIS and GPS PWV is presented in this section. In order to identify pixels with clear sky, the cloud mask product used had to indicate at least 95% confidence clear. It should be noted that all statistics were given after 2σ elimination, i.e. all differences more than twice the standard deviation were considered to be outliers and were removed. This elimination was mainly needed where poor collocations between the data in either time or space were found, or where cloudy pixels were falsely identified as cloud free.

Assuming the relationship between MODIS and GPS PWV to be linear, $\text{MODIS-PWV} = a \times (\text{GPS-PWV}) + b$, a least squares fit gave a scale factor of 1.05 ± 0.008 with a zero-point offset of -0.7 ± 0.1 mm and a standard deviation of 1.5 mm. The mean difference (MODIS – RS) PWV was 0.1 mm with a standard deviation of 1.6 mm. This suggests that MODIS appears to overestimate PWV over GPS with a scale uncertainty of 5%, which was consistent with its claimed accuracy of 5-10% [Gao *et al.*, 2003].

Taking into account the small standard deviation of the linear fit model, a linear correction model was proposed to calibrate MODIS PWV values as follows: $\text{MODIS-PWV (calibrated)} = 0.95 \times (\text{MODIS-PWV}) + 0.67$. Figure 3.b shows the inter-comparison between the calibrated MODIS PWV and GPS PWV after such a correction. The correlation coefficient increased from 0.96 to 0.97, and the

standard deviation of the mean difference decreased from 1.6 mm to 1.4 mm, indicating that the correction method was promising.

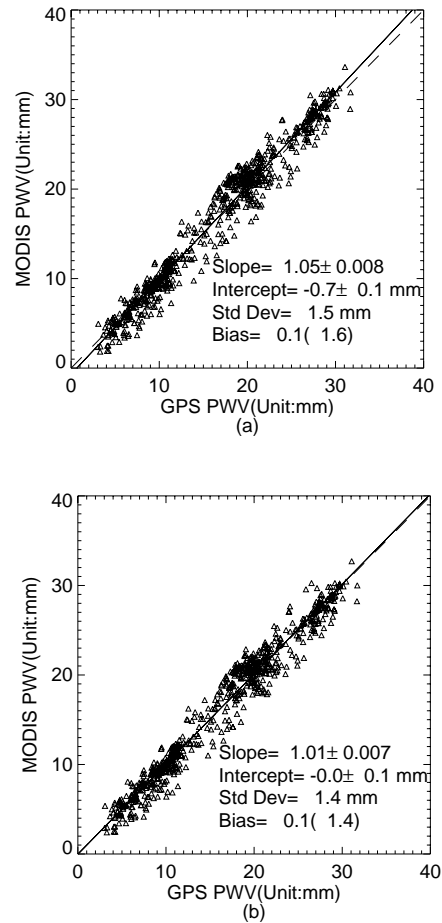


Figure 3. (a) Scatter plots of MODIS and GPS PWV under cloud-free conditions. The line of perfect fit (dashed line) and a least squares regression line (solid line) are plotted. The number of valid samples was 715, and 37 were omitted due to the 2σ exclusion. (b) Scatter plots of MODIS and GPS PWV under cloud-free conditions after applying the linear correction model.

4. DENSIFICATION OF MODIS NEAR IR WATER VAPOR FIELD

On the one hand, MODIS near IR water vapor is sensitive to the presence of clouds. On the other hand, both the frequency and the percentage of cloud free condition are only 15-30% on average at mid latitudes [Li *et al.*, 2004]. Therefore, there are often missing values in MODIS near IR water vapor field due to clouds, which limit its applications. In this section, an attempt is made to use an improved Inverse Distance Weighted interpolation (IIDW) to fill in these cloudy “missing” pixels.

The main steps are as follows: 1). MODIS PWV values under cloud free conditions were selected using cloud mask products, 2). Selected MODIS PWV values were

compared with GPS PWV values; 3). A correction model was derived from the inter-comparison; 4). This GPS-derived correction model was applied to calibrate MODIS PWV values; 5). An improved IDW was used to fill in cloudy pixels. It should be noted that Step 3 is optional if a GPS-correction model can be derived from a spatio-temporal inter-comparison (see Section 3), although an updated correction model on a case basis is optimal. The GPS-correction model was updated for each case in this study.

IDW assumes each measured pixel has a local influence on the predicted pixels that decreases with distance [Shepard, 1968]. It can be written as:

$$\left\{ \begin{array}{l} \hat{D}(\lambda_0, \varphi_0) = \sum_i w_i D(\lambda_i, \varphi_i) \\ w_i = \frac{d_{i0}^{-p}}{\sum_k d_{k0}^{-p}} \\ \sum_i w_i = 1 \end{array} \right. \quad (1)$$

where D are measured values, i.e. MODIS PWV values under cloud free conditions, \hat{D} is the predicted PWV value; λ and φ are longitude and latitude respectively; subscript 0 means the predicted value, subscript i means a measured value; d is the distance between the measured pixel and the “missing” pixel; p is a power parameter which influences the weighting of the predicted value. A lower power leads to a smoother surface and a high power results in a more detailed surface. A typical power parameter is 2.

Obviously, when the distance is large enough, water vapor values are uncorrelated with each other. *Emardson et al.* [2003] analyzed 126 GPS stations over SCIGN spanning the period from January 1998 to March 2000, and found that the water vapor variations were uncorrelated at distances greater than ~800 km (also see next Section). Therefore, an extent parameter d_{\max} was introduced to the traditional Inverse Distance Weighted interpolation (IDW), referred to as “improved IDW” (IIDW), in this paper: when d_{i0} was greater than d_{\max} , the weight was assigned to zero.

To apply the IIDW, a moving window was defined with a width of d_{\max} . The predicted surface is clearly smoother with a large width than that with a small width, which will be discussed later in this section. It is very likely that the quality of interpolation is dependent on the total number and the distribution of measured pixels in such a moving window. As a rule of thumb, only when the percentage of measured pixels was greater than 30% was IIDW applied to fill in the cloudy “missing” pixels in this paper.

$$\left\{ \begin{array}{l} \hat{D}(\lambda_0, \varphi_0) = \sum_i w_i D(\lambda_i, \varphi_i) \\ w_i = \frac{d_{i0}^{-p}}{\sum_k d_{k0}^{-p}} \quad (d_{i0} \leq d_{\max} \ \& \ d_{k0} \leq d_{\max}) \\ w_i = 0 \quad (d_{i0} > d_{\max}) \\ \sum_i w_i = 1 \end{array} \right. \quad (2)$$

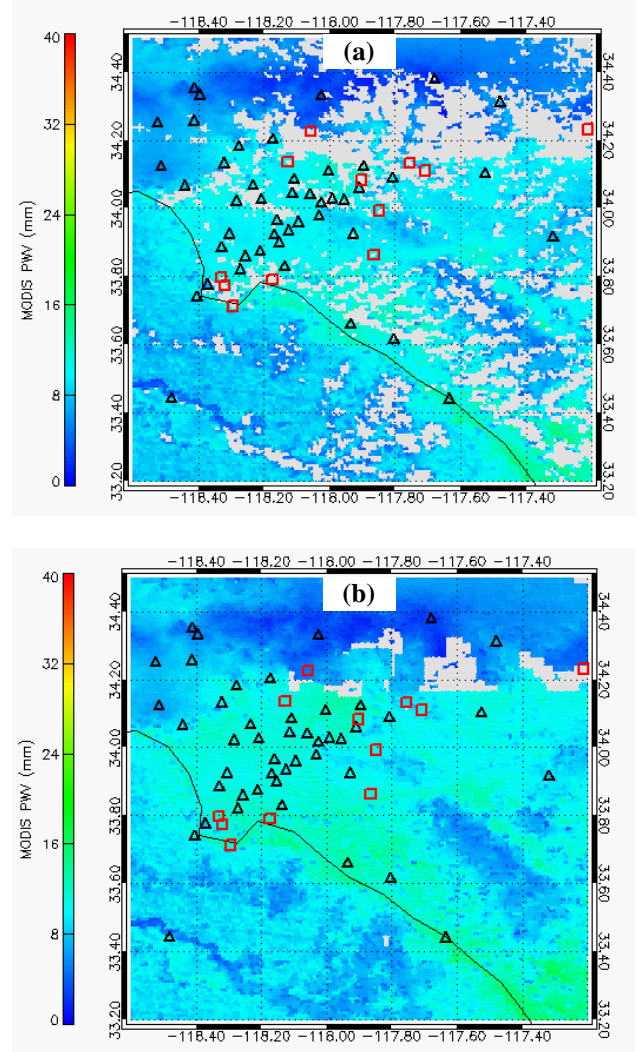


Figure 4. (a) MODIS near IR water vapor field collected at 18:50 UTC on 11 November 2000. Black triangles represent GPS stations under cloud free conditions, which were used to derive GPS correction model; Red squares represent GPS stations under cloudy conditions, which were used to validate the interpolated MODIS PWV values. (b) Densified MODIS near IR water vapor field after using the GPS-derived correction model.

Figure 4(a) shows the original MODIS near IR 2D water vapor field collected at 18:45 UTC on 11 November 2000, and Figure 4(b) shows the densified MODIS near IR 2D water vapor field corrected using GPS measurements. The

water vapor field initially had 75.9% coverage; following correction the water vapor field yielded 97.5% coverage, showing an absolute increase of 21.6% (Table 1).

In order to validate the densified 2D water vapor field, the densified (or interpolated) MODIS PWV values under cloudy conditions were compared with GPS PWV values (red squares in Figure 4). Table 1 shows the inter-comparisons between GPS and the densified MODIS PWV values before and after applying GPS-derived correction models. It is clear that both standard deviations and biases were closer to zero after correction, indicating that GPS-derived correction models were promising. It should be noted that only the data under cloudy conditions was used in the inter-comparisons after correction, implying that smaller biases and standard deviations could be achieved when including the data over cloud free pixels.

Table 1. Validation of the densified 2D MODIS near IR water vapor field ($p = 1$)

Date	Extent (km)	Before ^a Correction		After ^b Correction		Increased Coverage Percentage (%)
		Bias ^c (mm)	Std. (mm)	Bias ^c (mm)	Std. (mm)	
20001111	5	-0.5	1.2	0.1	0.9	21.6
	10	-0.6	1.2	0.0	0.8	22.9
20021012	5	-2.1	2.7	-1.0	1.6	14.2
	10	-2.1	2.6	-1.4	2.1	16.8

^a: Using data under cloud free conditions

^b: Using data under cloudy conditions

^c: Mean difference of (MODIS – GPS)

The impacts of the extent parameter d_{\max} on the interpolated values were also assessed in this study. When an extent parameter greater than 50 km was adopted, the predicted surface was too smooth and most of the detailed information was missing (not shown). Table 1 shows examples with extents of 5 km and 10 km. On the one hand, a larger extent always resulted in a larger increased coverage percentage. On the other hand, for Case 20001111, the extents of 5 km and 10 km resulted in similar standard deviations and biases, whilst the extent of 5 km led to a closer agreement with GPS PWV against the extent of 10 km after correction for Case 20001012. This also implies that a larger extent resulted in a smoother surface with a loss of some detailed information, which in turn indicates that the optimal extent parameter is different from the water vapor decorrelation range presented by *Emardson et al.* [2003].

It is noteworthy that the power parameter could be increased to reduce the influences of far pixels. Since several previous studies shows that water vapor variations conforms temporally and spatially to a power law process with an exponent varying continuously from around $5/3$ at small distances relative to heights to $2/3$ at large

distances [*Treuhaf and Lanyi, 1987; Williams et al., 1998; Emardson et al., 2003*] (also see Section 5), there is no obvious reason to adopt a power parameter greater than 2. A power parameter of 2 was also adopted to assess its impacts on interpolation, but no significant difference was observed between power parameters of 1 and 2 in both case studies (not shown in Table 1).

5. SPATIAL STRUCTURE OF WATER VAPOR

In order to describe the spatial variation of water vapor as a turbulent medium, a spatial structure function is usually applied. For a random function $x(\vec{O})$, where \vec{O} is a spatial coordinate, the spatial structure function for a displacement vector \vec{r} is defined as [*Tatarskii, 1971; Treuhaf and Lanyi, 1987; Williams et al., 1998*]:

$$D_x(\vec{O}, \vec{r}) = \left\langle \left[x(\vec{O} + \vec{r}) - x(\vec{O}) \right]^2 \right\rangle \quad (3)$$

where the angle brackets mean ensemble average. For homogeneous, isotropic and ergodic random fields, the spatial structure function depends only on the distance $r = |\vec{r}|$ and can be written as:

$$D_x(r) = D_x(\vec{O}, \vec{r}) \quad (4)$$

The spatial structure function is often described as a power law process [*Williams et al., 1998*]:

$$D_x(r) = C \times r^\alpha \quad (5)$$

where C characterizes the roughness or scale of the process, and α is the power index.

Based on this spatial structure function, *Treuhaf and Lanyi* [1987] developed a statistical model (TL hereafter) of water vapor fluctuations to yield wet tropospheric effects on very long baseline interferometry (VLBI). *Williams et al.* [1998] suggested that tropospheric variations in InSAR images conform temporally and spatially to the TL statistical model.

For the first time, the spatial structure functions were derived from MODIS near IR water vapor products (Figure 5). Although GPS-derived linear fit correction models only have an impact on the roughness parameter C , the calibrated MODIS near IR water vapor was used here. From Figure 5, it is clear that the spatial structure function was different from case to case. On the one hand, the water vapor variations in Case b (up to 60 mm^2 at a distance of about 200 km) was much greater than those in Case a (up to 40 mm^2 at a distance of about 600 km). On the other hand, $D_x(\vec{r})$ started to become relatively flat (despite the variation) from a distance of 200 km in Case

b, indicating that water vapor values are essentially spatially uncorrelated with distances greater than 200 km. However, in Case a, the spatial structure function increased smoothly until at a distance of about 600 km, suggesting that water vapor variations were somewhat correlated within this range of 600 km.

It should be noted that the power indices lay within $2/3$ to $5/3$ presented by *Treuhaft and Lanyi* [1987] in Case b, but the power index for distances larger than 10 km was slightly smaller than $2/3$ in Case a.

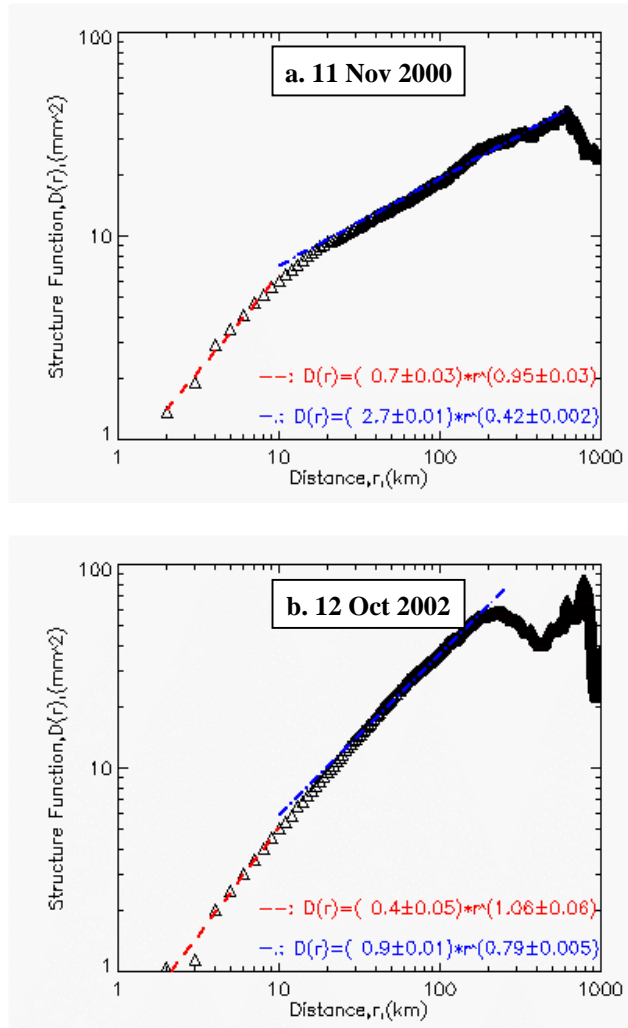


Figure 5. Spatial structure functions, $D_x(\vec{r})$, derived from MODIS near IR water vapor fields. The red dashed line represents the structure function for distances smaller than 10 km, and the blue dashed dot line for distances between 10 km and 600 km. a). Collected at UTC 18:45 on 11 November 2000; b). Collected at UTC 18:55 on 12 October 2002.

6. DISCUSSIONS AND CONCLUSIONS

The objective of this paper is to improve the spatial coverage and the accuracy of MODIS near IR water vapor

products (Collection 4) using GPS measurements. A spatial-temporal inter-comparison between MODIS and GPS PWV shows that MODIS appeared to overestimate PWV against GPS, with a scale factor of 1.05 and a standard deviation of 1.6 mm. After a linear fit model was applied, a better agreement between calibrated MODIS PWV and GPS PWV was achieved.

Since MODIS near IR water vapor is sensitive to the presences of clouds, an improved inverse distance weighted interpolation (IIDW) was proposed to fill in the cloudy pixels. The main drawbacks to the IIDW method are: 1). It is difficult to decide the optimal power parameter; 2). The optimal extent parameter is not the real water vapor decorrelation range, i.e., the extent parameter cannot represent a physical sense; 3). It does not take into account the height effects on water vapor variation. Despite these disadvantages, its applications to the calibrated MODIS water vapor field was promising: the densified MODIS PWV agreed with GPS PWV to 1.6 mm in terms of standard deviations, furthermore, the coverage of valid water vapor fields increased by 14.2% ~ 21.6%.

The spatial structure functions derived from MODIS near IR water vapor products showed that water vapor varied from time to time. Through the spatial structure analysis, it is also shown that the water vapor decorrelation range might as short as 200 km, which is different from the decorrelation range of 500-1000 km presented by *Emardson et al.* [2003] based on GPS data from Japan and radiosonde data from Europe. One possible cause for this discrepancy is the differences in the relative climates at different places and times. Another possible cause for this discrepancy lies in the high spatial resolution of the MODIS near IR water vapor fields, which leads to more detailed information on water vapor fields.

It is believed that the integration approach presented in this paper is very helpful when applying MODIS near IR water vapor products to correcting InSAR atmospheric effects. In our latest study, the integration approach presented here has been successfully incorporated into the JPL/Caltech ROI_PAC software, and its application to ERS-2 data over the Los Angeles SCIGN area shows this integration approach not only helps discriminate geophysical signals from atmospheric artefacts, but also reduces water vapor effects on SAR interferograms significantly [*Li et al.*, 2004].

It is worth mentioning that this approach could be applied to calibrate the ESA's MEdium Resolution Imaging Spectrometer (MERIS) near IR water vapor product, which has a potential to correct Advanced Synthetic Aperture Radar (ASAR) measurements [*Li et al.*, 2004]. The improvement of MERIS near IR water vapor products could lead to improved InSAR results.

ACKNOWLEDGMENTS

The author wishes to thank his supervisors, Prof. Jan-Peter Muller and Prof. Paul Cross, for their invaluable contributions. This research is supported by an Overseas Research Students Award (ORS) and a UCL Graduate School Research Scholarship. This work is also linked to the NERC Earth Observation Centre of Excellence: Centre for the Observation and Modelling of Earthquakes and Tectonics (COMET), and the ENVISAT project 853 (HAZARDMAP) which is co-funded by the European Commission Research Directorate-General 5th Framework Programme, Environment and Sustainable Development, Development of generic Earth observation technologies under the EU-CLOUDMAP2 project under contract EVG1-CT-2000-00033.

REFERENCES

- [1]. Bevis, M., S. Businger, T.A. Herring, C. Rocken, R.A. Anthes, and R. H. Ware, GPS Meteorology: Remote Sensing of Atmospheric Water Vapor Using the Global Positioning System, *Journal of Geophysical Research*, 97 (D14), 15,787-15,801, 1992.
- [2]. Emardson, T.R., M. Simons, and F.H. Webb, Neutral atmospheric delay in interferometric synthetic aperture radar applications: statistical description and mitigation, *Journal of Geophysical Research*, 108 (B5), 2231, doi:10.1029/2002JB001781, 2003.
- [3]. Gao, B.C., and Y.J. Kaufman, Water vapor retrievals using Moderate Resolution Imaging Spectroradiometer (MODIS) near-infrared channels, *Journal of Geophysical Research*, 108 (D13), 4389, doi:10.1029/2002JD003023, 2003.
- [4]. Li, Z., J.-P. Muller, and P. Cross, Comparison of precipitable water vapor derived from radiosonde, GPS, and Moderate-Resolution Imaging Spectroradiometer measurements, *Journal of Geophysical Research*, 108 (D20), 4651, doi:10.1029/2003JD003372, 2003.
- [5]. Li, Z., J.-P. Muller, P. Cross, P. Albert, J. Fischer, and R. Bennartz, Assessment of the potential of MERIS Near IR Water Vapour Products to Correct ASAR Interferometric Measurements, Submitted to *International Journal of Remote Sensing*, 2004.
- [6]. Li, Z., J.-P. Muller, P. Cross, and E. J. Fielding, InSAR atmospheric correction: II. GPS, MODIS and InSAR integration, Submitted to *Geophysical Research Letters*, 2004.
- [7]. Niell, A.E., A.J. Coster, F.S. Solheim, V.B. Mendes, P.C. Toor, R.B. Langley and C.A. Upham, Comparison of measurements of Atmospheric Wet Delay by Radiosonde, Water Vapor Radiometer, GPS, and VLBI, *Journal of Atmospheric and Oceanic Technology*, 18, 830-850, 2001.
- [8]. Shepard, D., A two-dimensional interpolation function for irregularly-spaced data, *Proc. 23rd National Conference ACM, ACM*, 517-524, 1968.
- [9]. Tatarskii, V.I., *The effects of the turbulent atmosphere on wave propagation*, 472 pp., Israel Program for Scientific Translations Ltd., 1971.
- [10]. Treuhaft, R.N., and G.E. Lanyi, The Effect of the Dynamic Wet Troposphere on Radio Interferometric Measurements, *Radio Science*, 22, 251-265, 1987.
- [11]. Webley, P.W., R.M. Bingley, A.H. Dodson, G. Wadge, S.J. Waugh, and I.N. James, Atmospheric water vapour correction to InSAR surface motion measurements on mountains: results from a dense GPS network on Mount Etna, *Physics and Chemistry of the Earth, Parts A/B/C*, 27 (4-5), 363-370, 2002.
- [12]. Williams, S., Y. Bock, and P. Fang, Integrated satellite interferometry: Troposphere Noise, GPS estimates, and implications for synthetic aperture radar products." *Journal of Geophysical Research*, 103(B11), 27051-27067, 1998.
- [13]. Zumbege, J.F., M.B. Heflin, D.C. Jefferson, and M.M. Watkins, Precise Point Positioning for the Efficient and Robust Analysis of GPS Data from Large Networks, *Journal of Geophysical Research*, 102 (B3), 5005-5017, 1997.